

Smart self-repairing protective coatings

Nanocontainers with a shell possessing controlled release properties can be used to fabricate a new family of active coatings that can respond quickly to changes in the coating environment or the coating's integrity. The release of corrosion inhibitors encapsulated within nanocontainers is triggered by the corrosion process, which prevents the spontaneous leakage of the corrosion inhibitor out of the coating. Moreover, if different types of nanocontainers loaded with the corresponding active agents are incorporated simultaneously into a coating matrix, the coating can act in several different ways (e.g. antibacterial, anticorrosion and antistatic). This review presents methods for the fabrication of such nanocontainers, how they can encapsulate active material, and their permeability properties.

Daria V. Andreeva* and Dmitry G. Shchukin

Max Planck Institute of Colloids and Interfaces, Am Mühlenberg 1, 14476 Golm, Germany

*E-mail: daria.andreeva@mpikg.mpg.de

A new generation of anticorrosion coatings that both possesses passive matrix functionality and actively responds to changes in the local environment has prompted great interest from material scientists. Corrosion is one of the most major destruction processes involved in material loss, and its prevention is paramount in protecting investments. Active corrosion protection aims to restore material properties (functionality) when the passive coating matrix is broken and corrosion of substrate has started. The coating has to release the active and repairing material within a short time after the coating integrity has been breached. This acts as a local trigger for the mechanism that heals the defect.

The oldest types of self-repairing coatings are polymer-based coatings. The concept of these coatings is as follows. Micrometer-scale containers, filled with monomers similar in nature to the polymer matrix and an appropriate catalyst or ultraviolet (UV)-sensitive agent to initiate the polymerization of the monomer when released at the damaged spot of the polymer coating, are incorporated inside the coating matrix. When these microcontainers become mechanically deformed, they release the monomer and catalyst and thus seal the defect¹. Repair of macroscopic adhesion defects formed throughout the service life of composites was carried out by filling hollow fibers with a polymer resin; these fibers would then fracture under excessive loading of the structure². The sealing component could be methyl

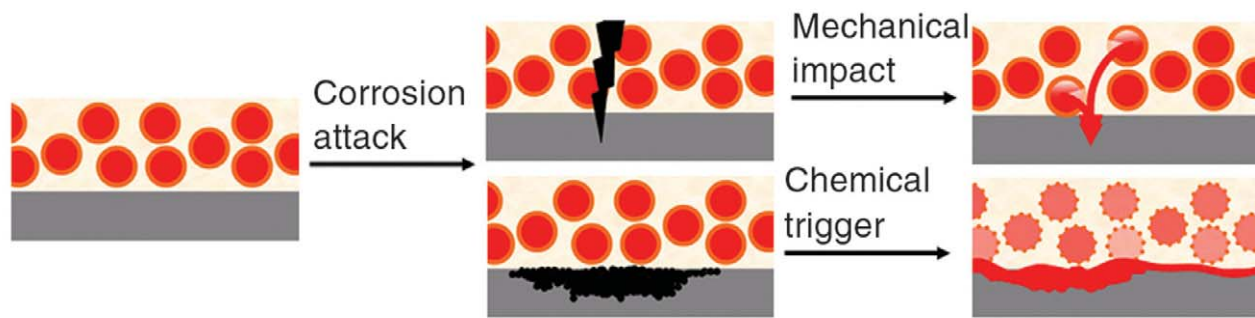


Fig. 1 The mechanism of self-healing action of a 'smart' anticorrosion coating.

methacrylate, 2-ethylhexyl methacrylate, tertiary butylaminoethyl methacrylate and lauryl methacrylate for fixing adhesion of the polypropylene matrix^{3,4}. Polyelectrolyte-based aqueous poly(L-lysine)-graft-poly(ethylene glycol) was employed as the self-healing agent in an oxide-based tribosystem⁵. The barrier properties of a damaged coating can also be recuperated by a simple blocking of the defects with insoluble precipitates.

Another approach to hybrid self-healing coatings is based on the use of inhibitors that can be released from the coating system. However, the direct introduction of inhibitor components into protective coatings very often leads to the deactivation of a corrosion inhibitor and degradation of the polymer matrix⁶. To overcome this, several systems entrapping the inhibitor and preventing its direct interaction with the coating matrix have been developed. One, quite simple, approach to inhibitor entrapment is based on the complexation of organic molecules by cyclodextrin⁷; another is based on the use of oxide nanoparticles, which can play the role of nanocarriers for corrosion inhibitors adsorbed on their surface. Immobilization of Ce^{3+} ions on the surface of ZrO_2 nanoparticles was achieved during the synthesis of a nano-sol by the controlled hydrolyzation of the precursor with a Ce-containing aqueous solution⁸. The inhibition of inorganic ions can also be incorporated by exchangeable ions associated with cation- and anion-exchange solids. Ca(II) and Ce(III) cation-exchanged bentonite anticorrosion pigments are prepared by the exhaustive exchange of naturally occurring bentonite⁹. For anion-exchange solids, the release of inhibitor anions can be provoked by aggressive corrosive chloride ions¹⁰.

The most important aspect in the design of new active coatings is to make nanocontainers that have good compatibility with the matrix components, that can encapsulate and maintain the active material, and that possess a shell with permeability properties that can be controlled by external stimuli. In order to develop functionalized micro- and nanocontainers, one has to combine several properties in the shell structure and composition. Depending on the nature of the 'smart' materials (e.g. polymers, nanoparticles) introduced into the container shell, various stimuli can induce reversible and irreversible shell modifications: pH, ionic strength, temperature, ultrasonic treatment, the presence of an alternating magnetic field or electromagnetic field.

The different responses that can be observed vary from fine effects, like tunable permeability, to more profound ones, like total rupture of the container shell. How a "smart" coating acts in response to a chemical trigger (pH, ionic strength) is shown schematically in Fig. 1.

Several approaches have been developed so far to fabricate micro- and nanocontainers¹¹. One approach is based on the self-assembly of lipid molecules or amphiphilic block copolymers into spherically closed bilayer structures (vesicles)^{12,13}. These relatively unstable structures then undergo cross-linking to stabilize the nanocontainer shell. A second approach is to use dendrimers or hyperbranched polymers as nanocontainers^{14,15}. However, in this case the particle preparation is a rather costly and time-consuming procedure, limiting any possible applications and scaling up. A third procedure involves suspension and emulsion polymerization around latex particles to form a cross-linked polymer shell. This method allows one to obtain hollow nanoshells from as small as 100 nm in a simple one-step procedure^{16,17}.

The approaches described above provide the general route for shell formation. The next step in the fabrication of nanocontainers suitable for self-repairing anticorrosion coatings is to make the nanocontainer shell sensitive to the corrosion process, or another external trigger, in order to activate the release of the encapsulated inhibitor species. This task can be achieved by employing the layer-by-layer (LbL) assembly approach in the formation of the nanocontainer shell¹⁸. This procedure entails the LbL deposition of charged species (e.g. polyelectrolytes, nanoparticles, biomaterials) as films on the surface of containers. Polyelectrolytes are macromolecules carrying a relatively large number of functional groups that are either charged or, under suitable conditions, can become charged. The molecules may be either polycations or polyanions, or both, depending upon the functional groups present^{19–21}. Polyelectrolyte films are able to change their chemical composition with pH since the degree of dissociation of the polyelectrolytes is pH sensitive. The films can be made to be richer in one polymer than in the other by working in a pH regime in which one of the polymers is weakly charged while the other is strongly charged. Thus, the polyelectrolyte composition can be prepared to be rich in the polycation or in the polyanion, or can be relatively equivalent in both. This property is exclusive to combinations of weak-weak and weak-strong polyelectrolytes. Active species deposited as a component of

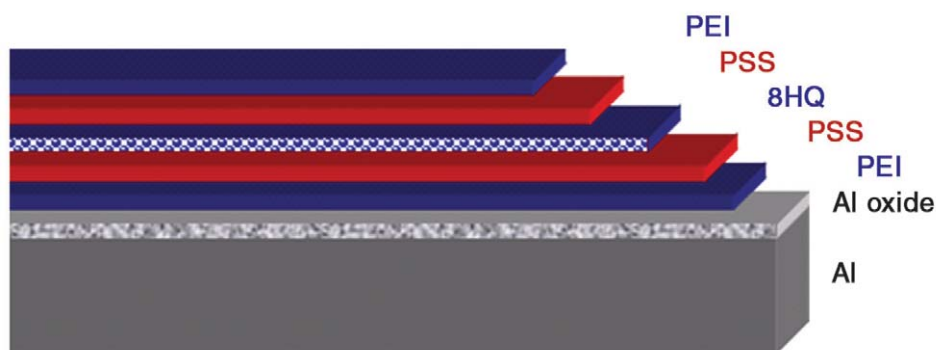


Fig. 2 The polyelectrolyte/inhibitor corrosion protection system on Al alloy.

the polyelectrolyte film are able to be released on demand. The shell of the resulting polyelectrolyte containers is semipermeable and sensitive to a variety of physical and chemical conditions (mechanical impact, change in pH) in the surrounding medium, enabling it to regulate the release of the entrapped inhibitor species. The mechanism of the smart self-healing process is shown in Fig. 1. Nanocontainers able to regulate the storage/release of an inhibitor can thus be constructed with nanometer-scale precision.

Polyelectrolyte multilayers

The self-repairing properties of the polyelectrolyte multilayer system are based on the following mechanisms: (i) the polyelectrolytes have pH-buffering activity and can stabilize the pH between 5 and 7.5 at the metal surface in corrosive media²²; (ii) the inhibitors are released from polyelectrolyte multilayers only after the start of the corrosion

process, preventing the corrosion from propagating directly in the damaged area; (iii) polyelectrolytes forming the coating are relatively mobile and have the ability to seal and eliminate the mechanical cracks of the coating²³. The design of our novel anticorrosion system is shown schematically in Fig. 2. The poly(ethyleneimine) (PEI, MW ~ 600–1000 kDa, Sigma-Aldrich), poly(styrene sulfonate) (PSS, MW ~ 70 kDa, Sigma-Aldrich) and corrosion inhibitor 8-hydroxyquinoline (8HQ)^{24–26} nanolayers are deposited on the pretreated Al alloy by spray drying from a 2 mg/ml solution of polyelectrolytes in a water/ethanol (1:1, v/v) mixture.

The scanning vibrating electrode technique (SVET) used allows current density maps over the selected surface of the sample to be measured, thus monitoring local cathodic and anodic activity in the corrosion zones²⁷. Aluminum plates covered by standard $\text{SiO}_x/\text{ZrO}_x$ sol-gel^{28–33} films were used to compare the efficiency

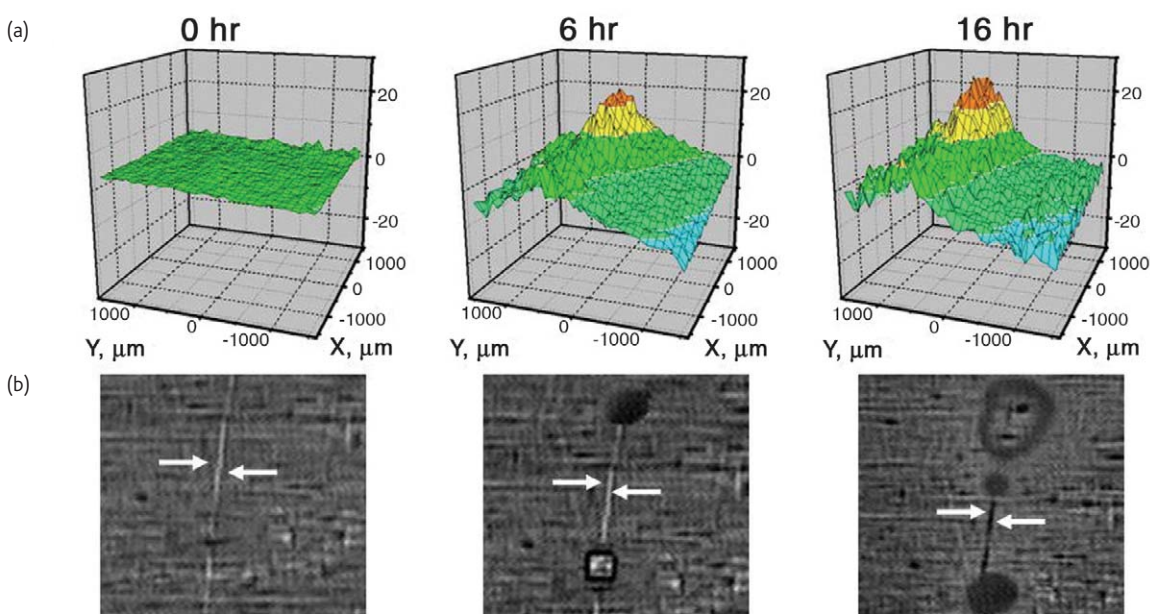


Fig. 3 (a) Scanning vibrating electrode measurements of the ionic currents above the surface of a scratched Al alloy covered by a standard sol-gel film (scale units: $\mu\text{A}/\text{cm}^2$; spatial resolution: $150\ \mu\text{m}$; solution: $0.1\ \text{M NaCl}$). (b) Photographs of the corrosion degradation of a scratched sol-gel film during the SVET experiment (the scratch is shown by the arrows). The contrast inversion from 6 to 16 h may be due to an increase in thickness caused by corrosion. (Reprinted with permission from²³. © 2008 Wiley-VCH.)

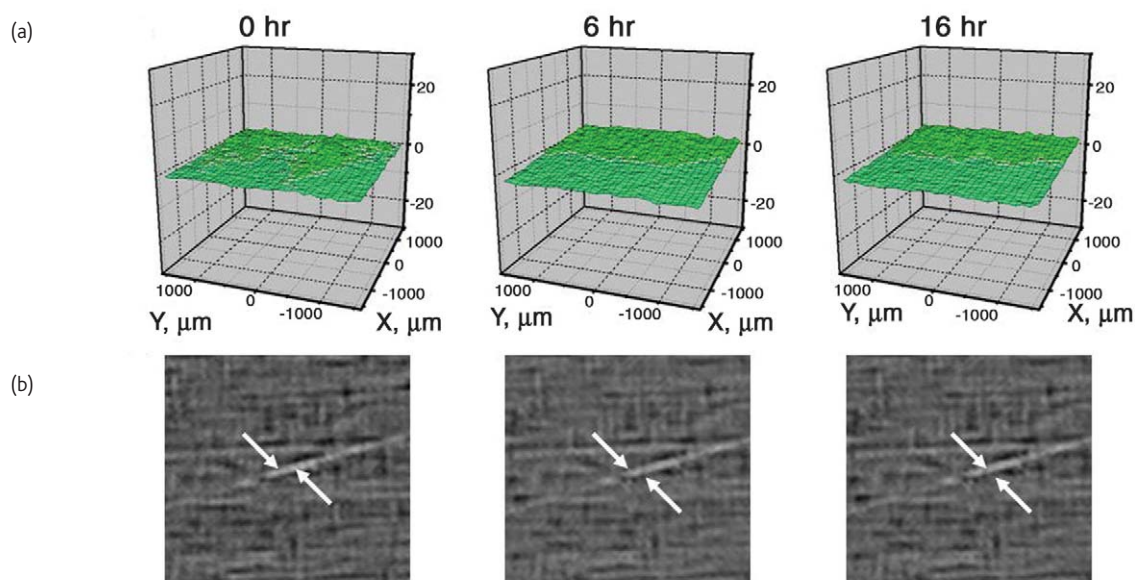


Fig. 4 (a) Scanning vibrating electrode measurements of the ionic currents above the surface of the scratched Al alloy covered by the polyelectrolyte/inhibitor coating (scale units: $\mu\text{A}/\text{cm}^2$; spatial resolution: $150\ \mu\text{m}$; solution: $0.1\ \text{M NaCl}$). (b) Photographs of the behaviour of the scratched surface during the SVET experiments (the scratch is shown by the arrows). (Reprinted with permission from Andreeva et al.²³ © 2008 Wiley-VCH.)

of polyelectrolyte-based coatings. Both coatings were mechanically scratched (2 mm long) (Figs. 3b and 4b) in order to stimulate the corrosion degradation of the Al surface and $0.1\ \text{M NaCl}$ solution was added immediately before the first scan. Fig. 3a shows the local current maps over the sol-gel-coated Al alloy surface. Well-defined anodic activity was observed on the Al surface immediately after immersion in the $0.1\ \text{M NaCl}$ solution. This activity became more intense with immersion time, resulting in the development of defects over the whole surface of the sample and ultimately to the total corruption of the Al surface.

The samples with polymer/inhibitor coating exhibited dramatically different behavior. Neither anodic activity nor corrosion products were observed for the experiment time of 16 h (Fig. 4a). It is amazing that even a 1-nm-thick polyelectrolyte/inhibitor coating provides effective corrosion protection for the Al alloy. The corrosion inhibitor incorporated as a component of the LbL film into the protective coating is responsible for this effective corrosion suppression. Both mechanical and polyelectrolyte swelling due to changes in local pH rupture the polyelectrolyte film, causing the localized release of the encapsulated inhibitor at the damaged part of the metal surface. Therefore, the inhibitor release occurs in response to the corrosion attack. This results in the termination of the corrosion process and the prolongation of corrosion protection. The long-term coating stability in a corrosive environment was studied by dipping the samples in aqueous NaCl solution at 20°C (Fig. 5). Corrosion defects could be observed after 12 h of immersion in $0.1\ \text{M NaCl}$ on unmodified Al (Fig. 5, right), whereas the sample with the polymer/inhibitor complex did not exhibit any visible signs of corrosion attack even after 21 days



Fig. 5 Long-term corrosion test: Al alloy covered by polyelectrolyte/inhibitor (left) and unmodified Al plate (right). (Reprinted with permission from Andreeva et al.²³ © 2008 Wiley-VCH.)

of immersion (Fig. 5, left). Furthermore, infrared spectra of the covered samples exhibited all the characteristic bands of the polymers and the inhibitor after dipping the protected Al plate in NaCl solution.

Nanocontainers inside the coating

Another approach for fabrication of feedback coatings is the use of natural or artificially synthesized inhibitor hosts. Halloysites (Fig. 6), which are one of the most abundant natural nanotubes, have recently been applied as containers in the automotive and maritime industries.

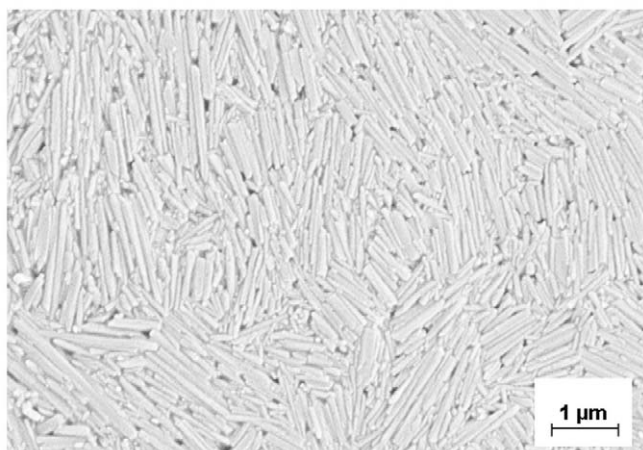


Fig. 6 Scanning electron microscopy image of halloysite nanotubes deposited onto an Al alloy surface.

The advantages of this type of container are its low price (approx. \$6.3 per kg) and the possibility of mining it by the ton. Halloysite is an aluminosilicate clay, up to 3.0 μm in length and with an outer diameter of up to 0.3 μm ³⁴. Due to the active surfaces and its particular shape, halloysite can be easily loaded with cationic compounds. The host (halloysite)–guest (loaded compounds) interaction is pH dependent. pH changes affect the complex stability and, therefore, trigger release of the loaded species. The pH sensitivity of halloysite can be enhanced by the formation of a pH-sensitive polyelectrolyte nanotube shell coating of retardant polymers following their saturation with corrosion inhibitor³⁵. To equip the halloysite nanotubes with controlled release properties, the surface of the nanotubes loaded with benzotriazole can be modified by the LbL deposition of polystyrene sulfonate/polyallylamine hydrochloride bilayers such that the openings at the edges became blocked with polyelectrolytes. Approximately 10% of the loaded material is released from halloysite nanotubes without a polyelectrolyte shell after 6 days of storage in neutral water. In contrast, the polyelectrolyte shell prevents any spontaneous release of the inhibitor, blocking the permeability of the halloysite nanotubes. The release of benzotriazole from halloysite nanotubes with a polyelectrolyte shell is triggered at pH 10. Loading of the halloysites with benzotriazole followed by the impregnation of nanotubes into a standard sol–gel ($\text{SiO}_x/\text{ZrO}_x$) coating results in the self-healing ability of the coating without any deterioration in the initial barrier properties of the sol–gel.

The anticorrosion activity of the halloysite/sol–gel hybrid coating was tested by SVET. A small amount of anodic activity was observed in the first 10 min (scanning time) after defect formation. However, after 3 h the surface showed negligible ion flux, indicating the absence of any corrosion processes. Therefore, the defected zone on the sol–gel coating was passivated by the release of the encapsulated inhibitor caused by the corrosion process, and there was no sign of the corrosion after 3 h of immersion.

The drawbacks of the natural nanotube halloysite lie in its poorly defined composition, its particle size, the size of its inner hollow lumen, and the presence of 10–20% of dense, non-hollow material in the commercial supply. These properties depend on the deposit of halloysite clay. To overcome these obstacles, if necessary, one can use mesoporous and microporous particles nearer to 100 nm in size as hosts for the entrapped inhibitor. These particles, mostly SiO_2 or TiO_2 , can be prepared via a large number of methods, as reported in the literature^{36–39}.

Mesoporous SiO_2 nanoparticles covered with polyelectrolyte layers and loaded with inhibitor (2-(benzothiazol-2-ylsulfanyl)-succinic acid) were randomly introduced into a hybrid ZrO_2 – SiO_2 sol–gel film. The spontaneous release of inhibitor was avoided by the formation of a polyelectrolyte shell over the container's outermost surface. Particles were prepared through sol–gel synthesis by adding tetraethoxysilane to ethanol solution, water and cetyltrimethylammonium bromide surfactant. The pore size covered a narrow range, of between 2 and 13 nm, with an average size of ~ 3 –4 nm. The polyelectrolyte shell was formed by the LbL deposition procedure. Positive polyethyleneimine was deposited first on the SiO_2 , followed by a negative polystyrene sulfonate layer. The inhibitor content in the nanocontainers was equal to 85 mg/g of the initial SiO_2 particles. The hybrid $\text{SiO}_x/\text{ZrO}_x$ sol–gel film with inhibitor-loaded SiO_2 containers was prepared by adding mesoporous SiO_2 to the mixture of sols followed by deposition onto the metal Al alloy by the dip-coating procedure. A uniform distribution of SiO_2 containers was achieved, with a distance between the containers of ~ 15 –20 nm.

The release of the 2-(benzothiazol-2-ylsulfanyl)-succinic acid from containers with a polyelectrolyte shell is triggered at pH 10. This effect is self-regulated and the inhibitor release takes place only in the region with the high pH, which triggers the self-healing process^{40–43}. When the pH returns to the initial value, the shell is closed and the release of the inhibitor stops. The SVET experiment shows that a self-healing ability can be achieved (Fig. 7). The corrosion activity was negligible at the beginning of the measurements, but appeared in the films both with and without inhibitor-loaded containers after 42 h (Fig. 7a). At the same time, the sol–gel films without the containers showed twice as much anodic activity ($\sim 20 \mu\text{A}/\text{cm}^2$) as those with them. The SVET measurements taken 60 h (Fig. 7b) after the start show that the anodic activity increased dramatically in the case of the sol–gel coating without the containers (large picture in Fig. 7b). In contrast, practical no corrosion was found at the surface of the coating with the containers (small picture in Fig. 7b).

Internal or external triggers other than pH can be used to trigger the release of inhibitor from nanocontainers incorporated into anticorrosion coatings. Examples include changes in the local electrochemical potential of the surface, heat, light, and humidity. The addition of a light-sensitive component (nanoparticles) into the polyelectrolyte-based nanocontainer shell would enable it to be

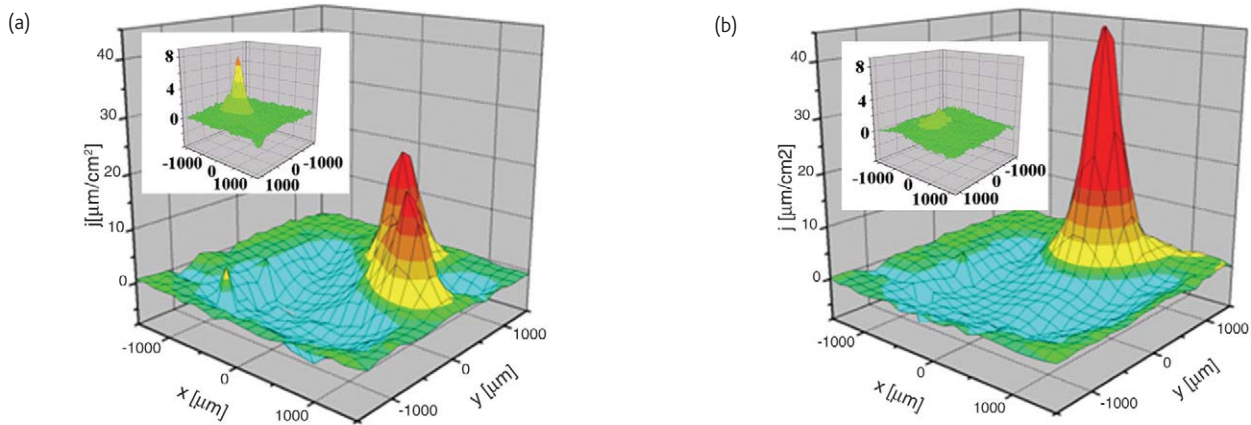


Fig. 7 Scanning vibrating electrode measurements of the ionic currents above the surface of the individual $\text{SiO}_x/\text{ZrO}_x$ hybrid film (the large pictures) and $\text{SiO}_x/\text{ZrO}_x$ hybrid film with inhibitor-loaded SiO_2 nanocontainers (the small pictures) after (a) 42 h and (b) 60 h of corrosion. Scale units: $\mu\text{A}/\text{cm}^2$; spatial resolution: $150 \mu\text{m}$; solution: 0.1 M NaCl .

opened under light irradiation of a specific wavelength, depending on the sensitivity of the additional component^{44–47}. If a scratch or other defect occurs, the illumination would ensure that the defect would be repaired.

One interesting approach to the fabrication of light-sensitive nanocontainers is based on the use of porous TiO_2 as a host for the incorporation of the inhibitor and of a polyelectrolyte shell to block any uncontrolled leakage from the mesopores. The aim of our study was to use UV light to open TiO_2 -based containers as traditional mesoporous containers are not sensitive to such irradiation. Benzotriazole was

loaded into TiO_2 as a corrosion inhibitor, and UV-induced shell oxidation and the release of inhibitor to restore the anticorrosion coating were studied. TiO_2 particles are $\sim 100 \text{ nm}$ in size, possess 5 nm pores, and have anatase crystal modification. The 365 nm line of a 120 W high-pressure Hg lamp was used for the UV activation of TiO_2 containers. The thickness of the obtained PEI/PSS polyelectrolyte shell was $\sim 10 \text{ nm}$. By this shell protection, no release of benzotriazole from TiO_2 containers was found if the surrounding environment was not changed. The inhibitor could be kept inside the containers until the moment of the UV irradiation.

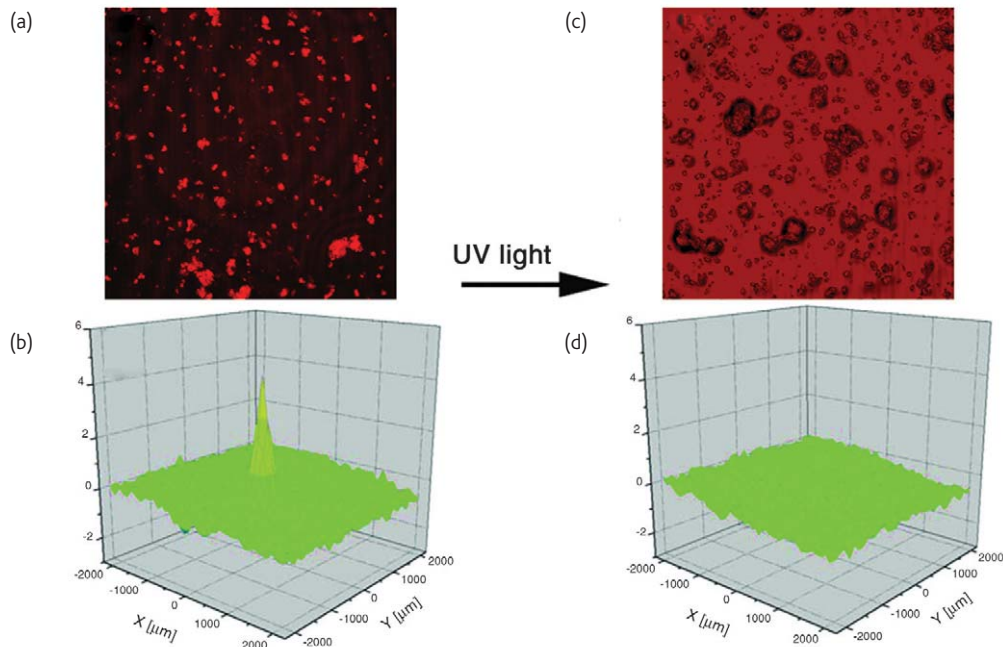



Fig. 8 Confocal images of polyelectrolyte containers with a TiO_2 core (in luminescent mode). The images are obtained (a) before and (c) after UV irradiation. The particles in the figures correspond to the aggregates of nanocontainers. Scanning vibrating electrode measurements of the ionic currents above the surface of polyelectrolyte– TiO_2 -based nanocontainers incorporated into $\text{SiO}_x/\text{ZrO}_x$ hybrid film (Al alloy is a substrate) (b) after 12 h of corrosion and (d) after UV irradiation and inhibitor release. Scale units: $\mu\text{A}/\text{cm}^2$; spatial resolution: $150 \mu\text{m}$; solution: 0.1 M NaCl .

The UV-activated opening of the TiO₂ containers and release of inhibitor results in the suppression of the corrosion process, as found by the SVET technique (Fig. 8a and c). After several hours in NaCl solution, anodic activity was observed (peak in Fig. 8b and d), which could be stopped after 5 min of irradiation. After local UV irradiation, any ongoing corrosion was suppressed completely. No such UV-stimulated fast healing was observed in the case of epoxy-functionalized SiO_x/ZrO_x sol-gel films without protective containers. Thus, for coatings where the very rapid but regulated release of inhibitor at a damaged corrosive area is necessary, the use of UV irradiation as an external trigger is a highly preferable option.

Conclusion and outlook

Nanocontainers possessing the ability to release encapsulated active materials in a controlled way can be employed to develop a new family of self-healing anticorrosion coatings. Several approaches to fabricate such self-healing coatings by the impregnation of sol-gel films with inhibitor-loaded polyelectrolyte multilayers, SiO₂ and TiO₂ containers, and halloysites have been demonstrated. Inorganic containers can be modified with a polyelectrolyte or polyelectrolyte/nanoparticle shell in order to provide them with permeability properties controlled by the changes in pH caused by corrosion or by external electromagnetic irradiation, whereas polyelectrolyte multilayers can be employed as an inhibitor storage nanonetwork without further modification. The release of the anticorrosion materials occurs only when triggered by

corrosion processes or focused light, which prevents leakage of the active component out of the coating.

The demonstrated approach to the fabrication of active coatings, on the other hand, faces the formidable challenge of developing multifunctional organic and composite nanocontainers that are able to encapsulate active material, retain it in their inner volume for a long period, and release it immediately on demand. Due to their low dimensionality and the semipermeable nature of their shell, nanocontainers can be employed in a variety of areas, such as drug delivery systems, nanoreactors, feedback-active surfaces, and fuel cells. In many cases, the detailed mechanisms of nanocontainer permeability are not yet well understood. Additional studies are required to investigate the kinetic and structural properties of the nanocontainer shell and the diffusion of the released active material inside the coating matrix. However, there is no doubt that nanocontainers will create countless new opportunities both in research and in technology for the fabrication of active composite materials. Regarding the possibility of up-scaling the production of inhibitor-loaded nanocontainers, the most promising candidates are natural halloysite nanotubes, which can be mined by the ton, or commercially available cheap mesoporous SiO₂ or TiO₂ particles. 

Acknowledgments

This work was supported by NanoFutur program of the German Ministry of Education and Research (BMBF).

REFERENCES

- Feng, W., et al., *Adv. Polym. Technol.* (2007) **26**, 1
- Li, W., and Calle, L. M., *Smart Coating for Corrosion Sensing and Protection, Proceedings of the US Army Corrosion Summit 2006*, Clearwater Beach, FL, Feb. 14–16 (2006)
- Davis, S. J., and Watts J. F., *J. Mater. Chem.* (1996) **6**, 479
- Allsop, N. A., et al., *Thermochim. Acta* (1998) **315**, 67
- Brown, E. N., et al., *J. Mater. Sci.* (2004) **39**, 1703
- Shchukin, D., et al., *Adv. Mat.* (2006) **18**, 1672
- Khramov, A. N., et al., *Thin Solid Films* (2004) **447–448**, 549
- Zheludkevich, M. L., et al., *Electrochim. Acta* (2005) **51**, 208.
- Buchheit, R. G., et al., *Corrosion* (2002) **58**, 3
- Leggat, R. B., et al., *Corrosion* (2002) **58**, 322
- Meier, W. *Chem. Soc. Rev.* (2000) **29**, 295
- Peyratout, C., et al., *Adv. Mater.* (2003) **15**, 1722
- Förster, S., and Plantenberg, T. *Angew. Chem. Int. Ed.* (2002) **41**, 689
- Manna, A., et al., *Chem. Mater.* (2001) **13**, 1674
- Sunder, A., et al., *Angew. Chem. Int. Ed.* (1999) **38**, 3552
- Lu, X., and Xin, Z. *Colloid Polym. Sci.* (2006) **284**, 1062
- Zoldesi, C.I., et al., *Langmuir* (2006) **22**, 4343
- Schneider, G., and Decher, G., *Nano Lett.* (2004) **4**, 1833
- Shiratori, S. S., and Rubner, M. F., *Macromolecules* (2000) **33**, 4213
- Dubas, S. T., and Schlenoff, J. B., *Langmuir* (2001) **17**, 7725
- DeLongchamp, D. M., and Hammond P. T., *Chem. Mater.* (2003) **15**, 1165
- Andreeva, D. V., et al., *J. Mater. Chem.* (2008) **18**, 1738
- Andreeva, D. V., et al., *Adv. Mater.* (2008) in press
- Garrigues, L., et al., *Electrochim. Acta* (1996) **41**, 1209
- Cicileo, G. P., et al., *Corros. Sci.* (1998) **40**, 1915
- Szunerits, S., Walt, D. R., *Anal. Chem.* (2002), **74**, 886
- He, J., et al., *J. Electrochem. Soc.* (2000) **147**, 3661
- Twite, R. L., and Bierwagen, G. P., *Prog. Org. Coat.* (1998) **33**, 91
- Brinker, C. J., and Scherer, G.W., *Sol-Gel Science*, Academic Press, San Diego, CA, (1990)
- Osborne, J. H., et al., *Prog. Org. Coat.* (2001) **41**, 217
- Voevodin, N. N., et al., *Prog. Org. Coat.* (2001) **41**, 287
- Yang, X. F., et al., *Surf. Coat. Technol.* (2001) **140**, 44
- Zheludkevich, M. L., et al., *Surf. Coat. Technol.* (2004) **200**, 3084
- Levis, S. R. and Deasy, P. B., *Int. J. Pharm.* (2002) **243**, 125
- Shchukin, D., and Möhwald, H., *Adv. Funct. Mater.* (2007) **17**, 1451
- Bruinsma, P.J., et al., *Chem. Mater.* (1997) **9**, 2507
- Lin, H.P., et al., *Chem. Mater.* (1998) **10**, 3772
- Hirashima, H., et al., *J. Non-Cryst. Solids* (2001) **285**, 96
- Zhao, J., et al., *Mater. Chem. Phys.* (2000) **63**, 9
- Zhang, W. L., and Frankel, G. S., *J. Electrochem. Soc.* (2002) **149**, 510
- Schmutz, P., and Frankel, G. S., *J. Electrochem. Soc.* (1998) **145**, 2295
- Zhang, W. L., and Frankel, G. S., *Electrochimica Acta* (2002) **48**, 1193
- Mansfeld, F., et al., *J. Electrochem. Soc.* (1998) **145**, 2792
- Skirtach, A. G., et al., *Angew. Chem. Int. Ed.* (2006) **45**, 4612
- Holmin, R. E., et al., *Angew. Chem. Int. Ed.* (2001) **40**, 2316
- von Klitzing, R., and Möhwald, H., *Langmuir* (1995) **11**, 3554
- Skirtach, A. G., et al., *J. Phys. Chem. C* (2007) **111**, 555